Time-resolved photoluminescence of $In_xGa_{1-x}N$/GaN multiple quantum well structures: Effect of Si doping in the barriers

C. K. Choi, Y. H. Kwon, B. D. Little, G. H. Gainer, and J. J. Song
Center for Laser and Photonics Research and Department of Physics, Oklahoma State University, Stillwater, Oklahoma 74078-0444

Y. C. Chang
Department of Physics and Materials Research Laboratory, University of Illinois at Urbana-Champaign, Urbana, Illinois 61801-3080

S. Keller, U. K. Mishra, and S. P. DenBaars
Electrical and Computer Engineering and Materials Department, University of California, Santa Barbara, California 93106
(Received 27 March 2001; revised manuscript received 31 July 2001; published 10 December 2001)

The carrier recombination dynamics in a series of $In_xGa_{1-x}N$/GaN multiple quantum wells, nominally identical apart from different Si doping concentrations in the GaN barriers, was studied by time-resolved photoluminescence (PL) with excitation densities ranging from 220 nJ/cm^2 to 28 μJ/cm^2 at 10 K and 300 K. At early time delays and with excitation densities greater than 5 μJ/cm^2, at which the strain-induced piezoelectric field is screened by both photogenerated carriers and electrons from the GaN barriers, we observe a strong $In_xGa_{1-x}N$ PL peak initially located $\sim$60 meV below the absorption edge and well above an effective mobility edge. This peak decays quickly with an effective lifetime less than 70 ps and disappears into the extended states while it gradually redshifts. The amount of this PL peak redshift decreases with increasing Si doping in the GaN barriers, suggesting that the peak is due to radiative recombination of free excitons in the screened piezoelectric field.

DOI: 10.1103/PhysRevB.64.245339 PACS number(s): 78.47.+p, 78.55.Cr, 71.35.−y, 77.65.Ly

Recent progress in the fabrication of InGaN/GaN multiple quantum well (MQW) devices has led to the blue laser diode with a lifetime of more than 10 000 h under continuous-wave operation at room temperature.[1] One characteristic property of this material system is a large Stokes shift between the absorption edge and the photoluminescence (PL) emission. This large Stokes shift has been attributed to (i) carrier localization due to potential fluctuations associated with the formation of In-rich areas or islands[2–7] and (ii) the presence of a strain-induced piezoelectric (PZ) field that leads to the quantum-confined Stark effect (QCSE).[8–11] It is of great interest to examine the electronic states and carrier recombination dynamics in samples free from the influence of the PZ effect. The PZ field can be screened out by both photogenerated carriers and extrinsic carriers in the InGaN active layer and/or the barriers. In the latter case, the extrinsic carriers originate from barrier impurity doping and move into the active layer to satisfy the requirement of a constant Fermi level across the layers. Compared to the case of impurity doping both in the well and the barriers, we expect a lower impurity-related PL emission in the barrier-only case. While the dependence of the optical, electrical, and structural properties of strained InGaN/GaN MQW structures on Si doping concentration has been extensively studied,[12–17] to the best of our knowledge, little information is known about the intrinsic excitonic recombination dynamics.

In this work, a set of $In_{0.18}Ga_{0.82}N$/GaN MQW structures with Si doping concentrations in the range of $1\times10^{17}-3\times10^{19}$ cm^{-3} in the GaN barriers has been studied by means of PL, PL excitation (PLE), and time-resolved PL (TRPL) to examine in detail the effect of Si doping on the optical properties. Special attention is paid to the recombination of free excitons in the InGaN active layers that is controlled by the screening of the PZ field.

The $In_{0.18}Ga_{0.82}N$/GaN MQW samples used in this work were grown on *c*-plane sapphire substrates by metalorganic chemical-vapor deposition (MOCVD). A set of samples, nominally identical apart from deliberate variations in the Si doping concentration (n_{Si}), were grown specifically to study the influence of Si doping in the GaN barriers. The samples consist of a 1.8-μm-thick GaN base layer and a 12-period MQW region with 3-nm-thick InGaN wells and 4.5-nm-thick GaN barriers, followed by an $Al_{0.07}Ga_{0.93}N$ capping layer. A detailed description of the growth conditions has been published elsewhere.[18] The Si doping concentrations, which were obtained from secondary-ion mass spectroscopy and Hall measurements, are 1×10^{17}, 2×10^{18}, and 3×10^{19} cm^{-3} for the different samples studied. A nominally undoped $In_{0.18}Ga_{0.82}N$/GaN epilayer sample used for comparison was grown by MOCVD at 800 °C. The structure consists of a 1.8 μm GaN layer on *c*-plane sapphire, a 50-nm-thick GaN:Si ($n_{Si}\sim10^{18}$ cm^{-3}) layer, followed by the 0.1 μm InGaN epilayer, and a 50-nm GaN:Si ($n_{Si}\sim10^{19}$ cm^{-3}) layer. To evaluate the interface quality and structural parameters, the samples were analyzed with four-crystal high resolution x-ray diffraction (HRXRD) using Cu $K\alpha_1$ radiation. The average InN molar fraction was measured by HRXRD, assuming Vegard's law. The angular distances between the satellite superlattice diffraction peaks and the GaN (0002) reflections were obtained by $\omega-2\theta$ scans. The spectra clearly showed higher-order satellite peaks, indicating high interface quality and good layer uniformity. The details of this x-ray analysis were reported elsewhere.[19]

The PL and PLE experiments were performed using quasimonochromatic light from a xenon lamp dispersed by a 0.5 m monochromator. TRPL spectroscopy was carried out

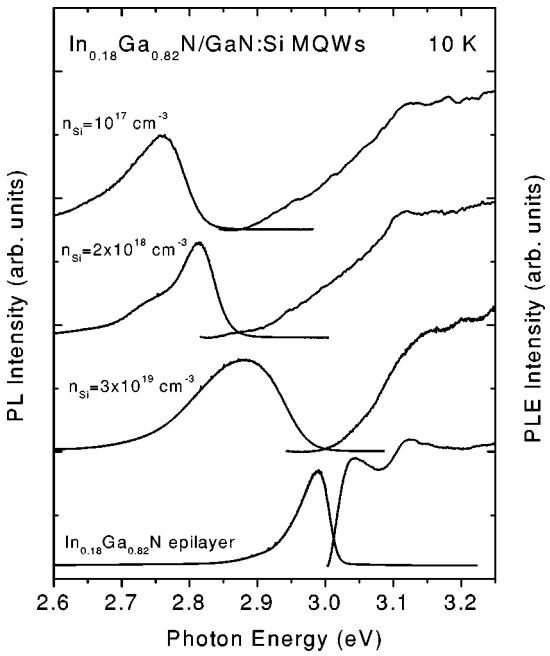

FIG. 1. PL and PLE spectra of a series of $In_{0.18}Ga_{0.82}N$/GaN MQW's and an $In_{0.18}Ga_{0.82}N$ epilayer at 10 K. The Si doping concentration in the GaN barriers of the MQW's ranged from 1×10^{17} to 3×10^{19} cm^{-3}. The Stokes shift of the PL peak with respect to the PLE band edge is seen to decrease with increasing Si doping concentration.

in the surface-emission geometry with a 1-kHz tunable femtosecond pulsed laser system for sample excitation and a streak camera for detection. The pulse duration time and output wavelength from the laser system were 355 fs (full width at half maximum) and 371 nm (3.342 eV), respectively. This allowed direct excitation of the InGaN QW's at 10 K and 300 K. The pump spot size was 150 μm in diameter and the overall time resolution for TRPL measurements was about 60 ps.

Figure 1 shows 10 K PL and PLE spectra of the main InGaN-related emission. The PLE detection energy was set at the main PL peak energy. For the nominally undoped (1×10^{17} cm^{-3}) sample, a large Stokes shift of $\sim$360 meV with respect to the band edge measured by PLE is observed. This Stokes shift decreases with increasing density of electrons from the Si donors in the GaN barriers and is found to be $\sim$250 meV for the heavily doped (3×10^{19} cm^{-3}) sample, in which a large screening of the PZ field is expected by the electrons even at low temperature. This indicates that the large Stokes shifts are probably due to the PZ field and large potential variations which result from In composition fluctuations, strain fluctuations, interface roughness, crystal dislocations, and other defects. The HRXRD measurements for these InGaN/GaN MQW's show that the Si doping in the GaN barriers significantly improves the structural and interface quality, although it does not change the overall strain state (i.e., it does not cause a relaxation of the lattice-mismatch induced strain).[19] Consistently, the reduced Stokes shift with increasing doping concentration also results from the band filling of localized states and better interface quality. The band edge of an InGaN/GaN MQW with Si doping in the GaN barriers is determined by a competition between the screening of the QCSE due to electrons from the GaN barriers and the 2-dimensional (2D) band gap renormalization (BGR) caused by the same carriers. Compared to the undoped MQW, the absorption edge of the heavily doped MQW is blueshifted by $\sim$20 meV. This could be due to the combination of phase-space filling, the QCSE, and BGR at $n_{Si}=3\times10^{19}$ cm^{-3}.

Neglecting the PZ field, alloy potential fluctuations, and spontaneous polarization we estimated the confinement energy levels in the $In_{0.18}Ga_{0.82}N$ QW's by a finite potential-well model. The electron and hole effective masses for the $In_{0.18}Ga_{0.82}N$ QW's are 0.2 m_e and 0.74 m_e, respectively, as estimated by a linear interpolation between the effective masses of 0.22 m_e and 0.8 m_e for GaN[20,21] and 0.12 m_e and 0.5 m_e for InN.[22] With a band gap energy difference of 450 meV between the GaN barrier (3.5 eV) (Ref. 23), and the $In_{0.18}Ga_{0.82}N$ epilayer (3.05 eV in Fig. 1) at 10 K and a conduction to valence-band offset ratio of 3:7 (measured by x-ray photoemission spectroscopy for the wurtzite crystal structure),[24] only the lowest confinement level ($n=1$) exists for electrons in the 3-nm-thick wells. The transition energy between the $n=1$ conduction and $n=1$ A-valence band levels at 10 K is estimated to be 3.14 eV, which is approximately equal to the PLE band edge of the heavily doped MQW sample and 20 meV larger than that of the undoped sample, as shown in Fig. 1. The 20 meV energy difference agrees well with theoretical calculations[11] of the redshift caused by the PZ field.[25]

Theses calculations and measurements show the basic trend that with increasing Si doping in the GaN barriers, the PZ field in the InGaN wells is screened more, causing a blueshift, although there is much uncertainty in the calculations and measurements due to factors, such as well thickness variations and In compositional fluctuation. In fact, we could not observe clear quantized state transitions in these MQW samples' photoreflection measurements, most likely because of the large band-gap inhomogeneity. We also performed a self-consistent calculation within the effective mass model (similar to that described in Ref. 26) to find the carrier distribution and potential profile for the modulation doped MQW's considered here. We found that, at 10 K and without the PZ field, the 2D carrier densities within each QW are about 4.5×10^{10}, 9×10^{11}, and 1.4×10^{12} cm^{-2}, respectively, for $n_{Si}=1\times10^{17}$, 2×10^{18}, and 3×10^{19} cm^{-3}. For the two samples with $n_{Si}\leqslant2\times10^{18}$ cm^{-3}, practically all the impurity electrons in the GaN barriers migrate to the QW's. For the heavily doped MQW sample at 10 K, only a fraction of the impurity electrons migrate into the QW's, while the rest of them remain at their impurity sites. In this case, the Fermi level is the same for the impurity electrons and the confined electrons. Under a strong PZ field ($\sim$1 MV/cm),[27] more impurity electrons migrate from the GaN base layer and the GaN barriers on the high potential side into the InGaN QW's (on the low potential side) and partially screen out the PZ field. This leads to a nonuniform distribution of carriers and different potential profiles for the 12 QW's.

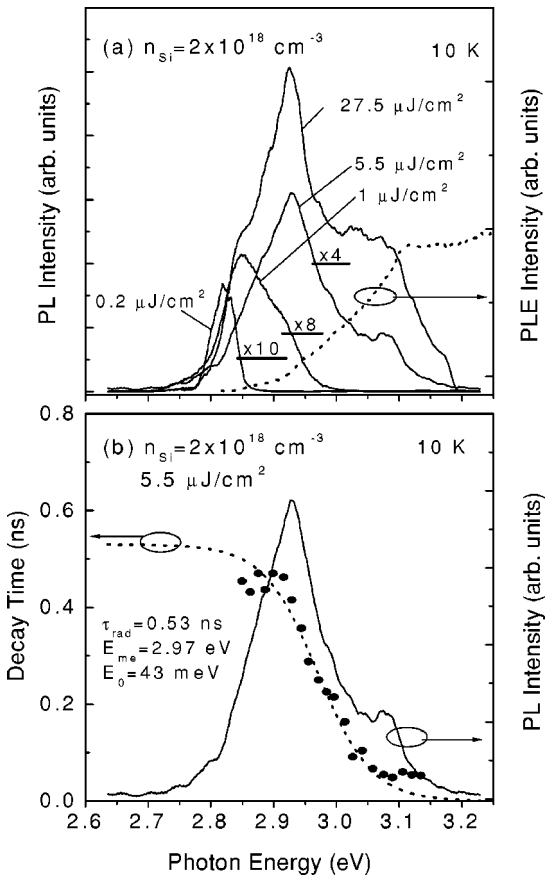

FIG. 2. (a) 10 K time-integrated PL spectra at various excitation densities for an $In_{0.18}Ga_{0.82}N$/GaN MQW with a Si doping concentration of 2×10^{18} cm^{-3} in the GaN barriers. The 10 K PLE spectrum is shown with a dashed line. (b) The effective recombination lifetime as a function of emission energy at an optical excitation density of 5.5 μJ/cm^2 for the same sample at 10 K. The solid and dotted curves are the corresponding time-integrated PL spectrum and the best fit to the equation $\tau(E)^{-1}=\tau_{rad}{}^{-1}(1+\exp[(E-E_{me})/E_0])$, respectively.

For the InGaN epilayer sample, we observe two peaks in the PLE spectrum (see Fig. 1). The low energy peak at ~3.04 eV corresponds to the bulk excitonic enhancement. The high energy peak at ~3.12 eV requires some explanation. Since the InGaN layer is between the heavily Si-doped GaN layers, charge transfer at the interfaces creates triangular QW's at the InGaN/GaN interfaces (refer to Fig. 1 in Ref. 26), and their first quantum confined level is about 80 meV above the sharp bottom of the deepest triangular QW. This 80 meV may account for the high-energy peak observed in the PLE spectrum.

Figure 2 shows (a) the optical excitation density dependence of the time-integrated PL spectra for the moderately doped MQW and (b) the spectral dependence of the PL decay time at an excitation density of 5.5 μJ/cm^2 at 10 K. At excitation densities less than 5.5 μJ/cm^2, the main PL peak blueshifts with increasing excitation density, mostly due to the band filling of localized states by the photogenerated carriers. For excitation densities higher than 5.5 μJ/cm^2, this PL peak slightly redshifts and narrows. A large increase in the effective recombination lifetime with decreasing energy across the main PL peak is shown in Fig. 2(b). This behavior can be well understood in terms of carrier (exciton) localization,[28–30] where the carrier decay is by radiative recombination and also by nonradiative transfer to deeper localized states through acoustic phonon-assisted relaxation or tunneling. Assuming the radiative decay time is independent of energy and the density of localized states is proportional to $[\exp(-E/E_0)]$ (E is the localization energy), we fit the experimental decay-time data to $\tau(E)^{-1}=\tau_{rad}{}^{-1}(1+\exp[(E-E_{me})/E_0])$,[30] where τ_{rad} is the radiative lifetime, E_{me} is the energy analogous to a mobility edge,[31] and E_0 is the characteristic energy describing the energy dependence of the density of states. The best fit was obtained for $\tau_{rad}=0.53$ ns, $E_{me}=2.97$ eV, and $E_0=43$ meV. For the undoped and heavily doped MQW's at the same excitation density, we obtained τ_{rad} values of 1.95 and 0.57 ns, E_{me} values of 2.90 and 2.99 eV, and E_0 values of 35 and 45 meV, respectively. The blueshift of the mobility edge with increasing Si doping concentration is consistent with the reduction of the Stokes shift.

We note that at higher excitation densities, the time-integrated spectra of Fig. 2(a) contain two peaks. As the excitation density is increased from 5.5 μJ/cm^2 to 27.5 μJ/cm^2, the higher-energy peak, which occurs ~60 meV below the estimated lowest quantum-confined transition energy of 3.14 eV, rises much faster than the lower energy main PL peak and decays fast with a recombination lifetime of 70 ps, as shown in Fig. 2(b). At early time delays for the three different Si doping concentrations in the GaN barriers, the temporal evolution of this high-energy PL peak at an excitation density of 27.5 μJ/cm^2 is shown in Fig. 3. The second curve from the bottom on each graph is taken at the peak of the TRPL decay curve. The bottom curve is at the time delay that has an intensity $1/e$ times the peak intensity. For the heavily and moderately doped MQW's, the high-energy peak initially occurs at 3.08 eV, and then redshifts 6 and 16 meV, respectively, by the time the TRPL decay curve reaches its maximum intensity. On the other hand, for the undoped MQW, the high-energy peak initially occurs at 3.04 eV, and then redshifts 37 meV by the time the TRPL reaches maximum intensity. For all three MQW's, the high-energy peak does not gradually redshift to the main PL peak, which is located below the mobility edge. Rather, this high-energy peak disappears into the extended states, leaving only a shoulder on the main PL peak, as shown in the bottom curve on each graph in Fig. 3. This behavior indicates that the high-energy peak is related to radiative recombination of an intrinsic bound state controlled by the QCSE.

This high-energy peak is attributed to the recombination of the $n=1$ A and B excitons, which are related to the $\Gamma_9^V-\Gamma_7^C$ and Γ_7^V (upper band)$-\Gamma_7^C$ interband transitions in the InGaN layer, respectively. The large strain-induced PZ field perpendicular to the QW layers (~1.2 MV/cm for a similar undoped sample, according to Ref. 27) is much larger than the classical exciton ionization field of 6.5×10^4 V/cm $[=E_B/ea_B$, where E_B is the zero-field exciton binding energy of 22 meV and a_B is the excitonic Bohr radius of 3.4

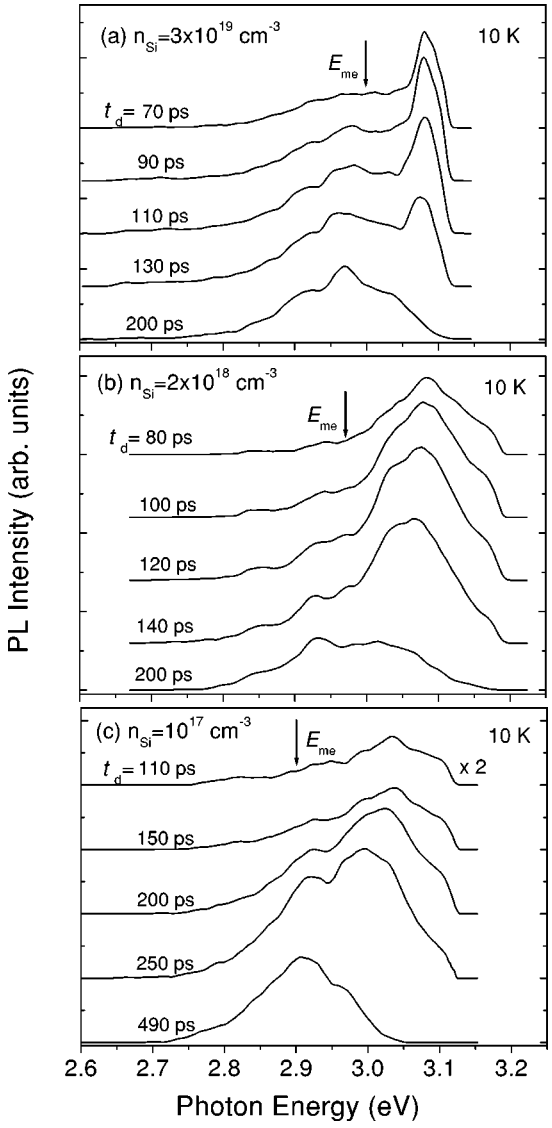

FIG. 3. Time-resolved PL spectra of $In_{0.18}Ga_{0.82}N/GaN$ MQW's with GaN barrier Si doping concentrations of (a) 3×10^{19}, (b) 2×10^{18}, and (c) 1×10^{17} cm^{-3} at an excitation density of 27.5 μJ/cm^2 and 10 K, showing the screening of the piezoelectric field by electrons from Si donors in the GaN barrier and by photogenerated carriers. The arrows indicate the effective mobility edge for each sample. The PL curves are displaced vertically for clarity.

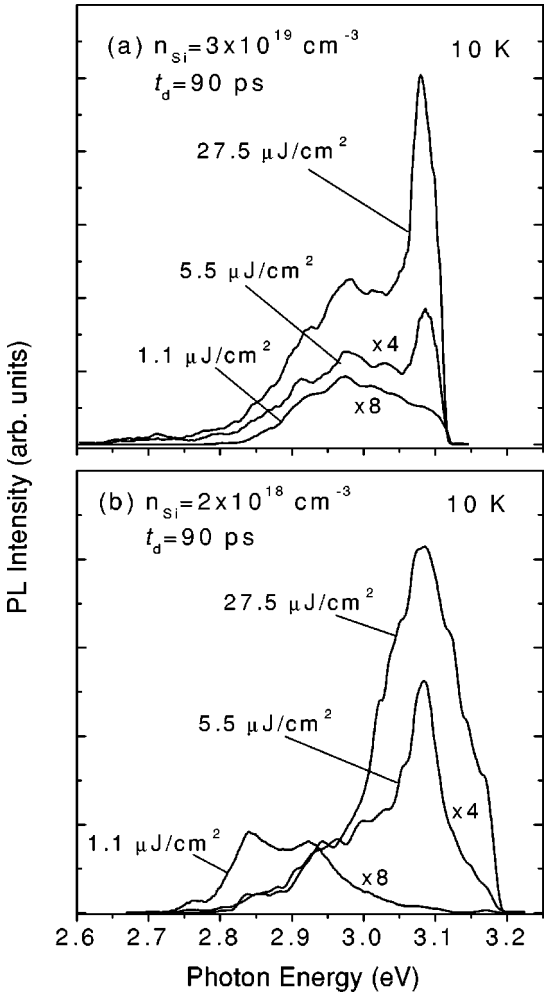

FIG. 4. PL spectra at a time delay of $t_d=90$ ps for the $In_{0.18}Ga_{0.82}N/GaN$ MQW's with Si doping concentrations of (a) 3×10^{19} and (b) 2×10^{18} cm^{-3} in the GaN barriers at the indicated optical excitation densities and at 10 K.

nm in GaN (Ref. 23)]. Therefore, the PZ field separates the electron-hole pairs and drastically reduces their overlap integral at low carrier densities. The average areal carrier density at an excitation power density of 27.5 μJ/cm^2 is estimated to be 1.4×10^{12} cm^{-2} (7×10^{18} cm^{-3} in 3D). This value is below the Mott density in GaN, which is given in the first approximation by $n_M=1/\pi(a_B^{2D})^2=1.1\times10^{13}$ cm^{-2}, where $a_B^{2D}(=a_B/2)$ is the 2D Bohr radius of the exciton. Immediately after excitation, a large number of photogenerated excitons and the electrons from the GaN barriers screen the PZ field. As radiative recombination proceeds, the screening effect is reduced and the transition energies as well as the oscillator strength of excitons are lowered. When the field ionization is dominant over the screening effect, the excitons cannot exist any longer. Thus, the temporal behavior of the high-energy PL peak shown in Fig. 3 may be understood as QCSE-controlled excitonic recombination. Previously, an electric field applied perpendicular to the plane of a GaAs/AlGaAs QW sample was shown to redshift the excitonic absorption peak by up to 2.5 times the zero-field binding energy. This redshift was observed for an applied field strength of 50 times the ionization field—the maximum field at which the excitons could still be resolved.[25] Compared to the exciton peak position in the moderately and heavily doped MQW's, the exciton peak in the undoped MQW is redshifted by 40 meV. With an estimated carrier density of 7×10^{18} cm^{-3}, the PZ field still exists in the undoped sample and causes a redshift of its excitonic transition. It has been reported that the exciton binding energy in GaAs/AlGaAs QW's increases with decreasing well thickness and is only about two times the 3D value when the well thickness is the same as the 3D Bohr radius.[32,33] Since the InGaN/GaN MQW samples studied here have a 3 nm well thickness, which is less than the GaN exciton Bohr radius, an exciton binding energy of 60 meV in the well at zero PZ field is

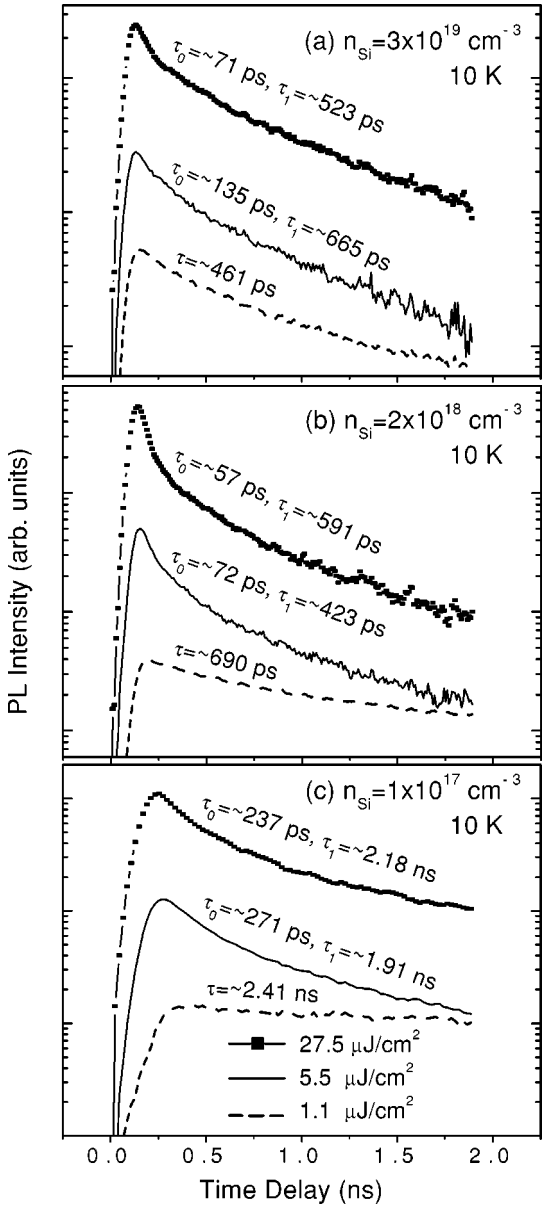

FIG. 5. Time decays of the whole InGaN PL peak of $In_{0.18}Ga_{0.82}N$/GaN MQW's with Si doping concentrations of (a) 3×10^{19}, (b) 2×10^{18}, and (c) 1×10^{17} cm^{-3} in the GaN barriers, at the designated excitation densities. The indicated effective recombination lifetimes were obtained by curve fitting to double (for excitation densities of 27.5 and 5.5 μJ/cm^2) and single (for 1.1 μJ/cm^2) exponential decays.

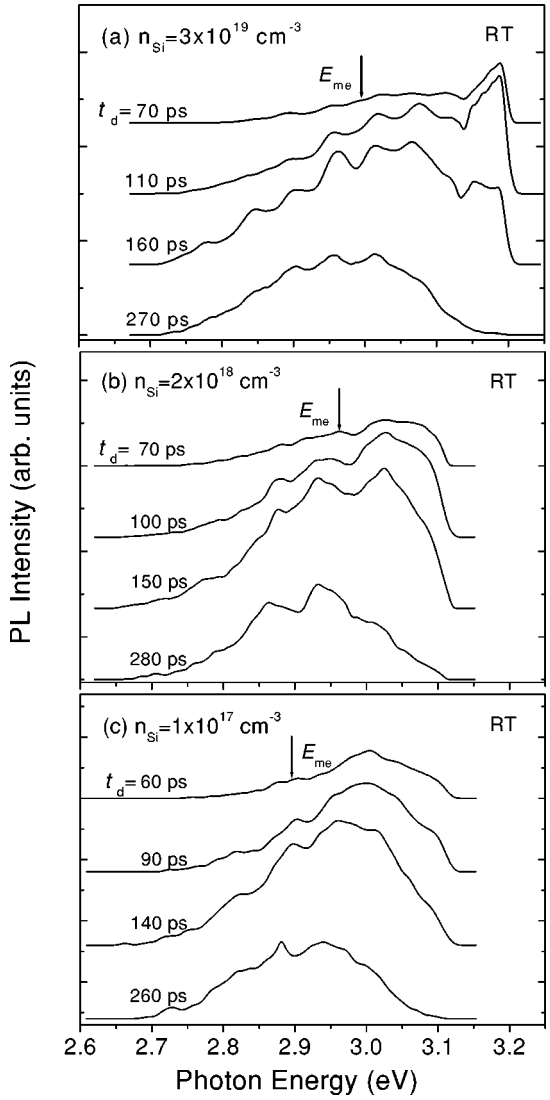

FIG. 6. Time-resolved PL spectra of the $In_{0.18}Ga_{0.82}N$/GaN MQW's with Si doping concentrations of (a) 3×10^{19}, (b) 2×10^{18}, and (c) 1×10^{17} cm^{-3} in the GaN barriers at an optical excitation density of 27.5 μJ/cm^2 at room temperature. The arrows indicate the effective mobility edge for each sample at RT. The PL curves are displaced vertically for clarity.

reasonable for our InGaN/GaN MQW's.

Although the temporal behavior of the excitonic PL peak can be well explained in terms of the PZ field-induced QCSE, the time-integrated PL of InGaN/GaN MQW's is quite different from that of GaAs/AlGaAs MQW's. Since the band tail states are much larger in an InGaN ternary alloy than in pure GaAs, the excitons in InGaN/GaN QW's nonradiatively transfer to the deeper localized states. As seen in Fig. 2(a), even at an excitation density of 27.5 μJ/cm^2, most of the photoexcited carriers radiatively recombine from deep localized states with a transition energy of ~2.92 eV instead of from the exciton levels with a transition energy of ~3.08 eV. The much shorter effective lifetime of the excitonic transition shows that the exciton recombination lifetime of 70 ps is dominated by a short nonradiative component.

The excitation power density dependence of the PL spectra for the (a) heavily and (b) moderately doped samples at 10 K and 90 ps time delay is shown in Fig. 4. With decreasing excitation density, a rapid reduction in the excitonic transition intensity is observed in both cases as a result of field ionization. At the lowest excitation density of 1.1 μJ/cm^2 in Fig. 4(a) for the heavily doped sample, we cannot see an appreciable PL peak from excitonic recombination. Thus, the InGaN carrier density is too low at this excitation density to screen the PZ field, which significantly reduces the oscillator strength of excitons. This indicates that most of the electrons remain trapped at the GaN:Si donor sites with only a small

fraction migrating into the InGaN active layer at 10 K, even for a Si doping concentration of 3×10^{19} cm^{-3} in the GaN barriers. The excitonic PL peak linewidth at an excitation density of 27.5 $\mu J/cm^2$ in Fig. 3(b) is much broader than in Fig. 3(a). At this excitation density in both samples, we expect the PZ field to be screened out by the photogenerated carriers and the electrons from the GaN barriers. We found that the optical properties of the samples studied here are not consistent with their structural quality. The maximum luminescence intensity and the lowest stimulated emission threshold by nanosecond pulse excitation in the side pumping geometry were observed for the moderately doped sample, which means it possesses the highest quantum efficiency among the three samples studied here.[7] Thus, at the same excitation density, the broader exciton PL linewidth in the moderately doped sample is mainly due to the substantially larger number of photogenerated electron-hole pairs. The broadening of the exciton PL peak in Fig. 4(b) is also ascribed to the larger alloy and layer thickness fluctuations in the moderately doped MQW than the heavily doped one, which is consistent with HRXRD measurements for these MQW's.[19]

Figure 5 shows the PL time decays (of the whole InGaN peak) with indicated effective lifetimes determined by single (for an excitation density of 1.1 $\mu J/cm^2$) and double (for 5.5 and 27.5 $\mu J/cm^2$) exponential fittings for the (a) heavily doped, (b) moderately doped, and (c) undoped InGaN/GaN MQW's. For the 5.5 and 27.5 $\mu J/cm^2$ excitation densities, the first decay component results from fast exciton recombination, while the second component corresponds to localized carrier recombination which results in the main PL peak. Compared to Figs. 5(a) and 5(b), the longer effective exciton lifetimes in Fig. 5(c) result from a reduction in oscillator strength caused by the PZ effect, as shown in Fig. 3. The undoped MQW has a much longer localized carrier lifetime than the heavily and moderately doped MQW's. This can be attributed to larger degree of localization and a smaller density of electrons from the Si donors in the GaN barriers.

Because the Si shallow donor level has an ionization of energy of only $\sim$22 meV,[34] at room temperature (RT), a large number of thermally activated electrons in the GaN barriers migrate into the InGaN active layer to satisfy the requirement of a constant Fermi level across the layers, especially for the heavily doped MQW's. In the TRPL measurement of the heavily doped MQW at RT and at an excitation density of 27.5 $\mu J/cm^2$, we could not observe the pronounced excitonic PL peak shown in Fig. 3(a), because strong screening by the migrated electrons would prohibit the formation of the excitons. Instead, we observe a broad peak at higher energies (ranging from 3.14 to 3.18 eV), as shown in Fig. 6(a). The onset of this peak is close to the 10 K band edge of 3.14 eV, indicating that it is due to unbound states. We, therefore, attribute this peak to recombination of the high-density electron plasma (due to doping) with the photogenerated holes.

The exciton recombination behavior at RT and at an excitation density of 27.5 $\mu J/cm^2$ for moderately doped and undoped MQW's is shown in Figs. 6(b) and 6(c). Their behavior is similar to that at 10 K shown in Figs. 3(b) and 3(c). By the same method used for 10 K, the lowest transition energy between the $n=1$ conduction and $n=1$ A-valence band levels at RT is estimated to be 3.07 eV, which is $\sim$40 meV larger than the exciton PL peak in Fig. 6(b). The RT exciton PL peak intensity is relatively weaker than that at 10 K, at the same excitation density, most likely due to thermal dissociation.

In conclusion, we have systematically investigated the carrier recombination properties of a series of $In_{0.18}Ga_{0.82}N$/GaN:Si MQW structures with different Si doping concentrations in the GaN barriers, using TRPL at various excitation power densities. At excitation densities greater than 5 $\mu J/cm^2$, a strong excitonic PL peak in the extended states is observed for all three MQW's and its temporal evolution as a function of the GaN barrier Si doping is well described by a QCSE-controlled excitonic recombination mechanism. When the PZ field is almost screened by photogenerated carriers and by the electrons from the Si donors in the GaN barriers, the excitonic PL peak at 10 K is located $\sim$60 meV below the band edge determined by PLE measurements for the $In_{0.18}Ga_{0.82}N$ (3 nm)/GaN (4.5 nm) MQW's studied here.

This work was supported by BMDO, AFOSR, ONR, and NSF.

[1] S. Nakamura, M. Senoh, S. Nagahama, N. Iwasa, T. Yamada, T. Matsushita, H. Kiyoku, Y. Sugimoto, T. Kozaki, H. Umemoto, M. Sano, and K. Chocho, Appl. Phys. Lett. **72**, 211 (1998).

[2] S. Chichibu, T. Azuhata, T. Soda, and S. Nakamura, Appl. Phys. Lett. **69**, 4188 (1996).

[3] M. Smith, G. D. Chen, J. Y. Lin, H. X. Jiang, M. A. Khan, and Q. Chen, Appl. Phys. Lett. **69**, 2837 (1996).

[4] Y. Narukawa, Y. Kawakami, Sz. Fujita, Sg. Fujita, and S. Nakamura, Phys. Rev. B **55**, 1938 (1997).

[5] A. Satake, Y. Masumoto, T. Miyajima, T. Asatsuma, F. Nakamura, and M. Ikeda, Phys. Rev. B **57**, 2041 (1998).

[6] K. P. O'Donnell, R. W. Martin, and P. G. Middleton, Phys. Rev. Lett. **82**, 237 (1999).

[7] Y.-H. Cho, T. J. Schmidt, S. Bidnyk, G. H. Gainer, J. J. Song, S. Keller, U. K. Mishra, and S. P. DenBaars, Phys. Rev. B **61**, 7571 (2000).

[8] T. Takeuchi, S. Sota, M. Katsuragawa, M. Komori, H. Takeuchi, H. Amano, and I. Akasaki, Jpn. J. Appl. Phys., Part 2 **36**, L382 (1997).

[9] S. F. Chichibu, A. C. Abare, M. S. Minsky, S. Keller, S. B. Fleischer, J. E. Bowers, E. Hu, U. K. Mishra, L. A. Coldren, and S. P. DenBaars, Appl. Phys. Lett. **73**, 2006 (1998).

[10] A. Hangleiter, J. S. Im, H. Kollmer, S. Heppel, J. Off, and F. Scholz, MRS Internet J. Nitride Semicond. Res. **3**, 15 (1998).

[11] E. Berkowicz, D. Gershoni, G. Bahir, E. Lakin, D. Shilo, E. Zolotoyabko, A. C. Abare, S. P. DenBaars, and L. A. Coldren,

Phys. Rev. B **61**, 10 994 (2000).
[12] T. Deguchi, A. Shikanai, K. Torii, T. Sota, S. Chichibu, and S. Nakamura, Appl. Phys. Lett. **72**, 3329 (1998).
[13] S. Chichibu, D. A. Cohen, M. P. Mack, A. C. Abare, P. Kozodoy, M. Minsky, S. B. Fleischer, S. Keller, J. E. Bowers, U. K. Mishra, L. A. Coldren, D. R. Clarke, and S. P. DenBaars, Appl. Phys. Lett. **73**, 496 (1998).
[14] Y. Yamada, T. Taguchi, F. Sasaki, S. Kobayashi, and T. Tani, J. Cryst. Growth **189/190**, 611 (1998).
[15] Y.-H. Cho, J. J. Song, S. Keller, M. S. Minsky, E. Hu, U. K. Mishra, and S. P. DenBaars, Appl. Phys. Lett. **73**, 1128 (1998).
[16] J. Dalfors, J. P. Bergman, P. O. Holtz, B. E. Sernelius, B. Monemar, H. Amano, and I. Akasaki, Appl. Phys. Lett. **74**, 3299 (1999).
[17] T. Wang, H. Saeki, J. Bai, T. Shirahama, M. Lachab, S. Sakai, and P. Eliseev, Appl. Phys. Lett. **76**, 1737 (2000).
[18] S. Keller, A. C. Abare, M. S. Minsky, X. H. Wu, M. P. Mack, J. S. Speck, E. Hu, L. A. Coldren, U. K. Mishra, and S. P. DenBaars, Mater. Sci. Forum **264-268**, 1157 (1998); B. P. Keller, S. Keller, D. Kapolnek, W. N. Jiang, X. -F. Wu, H. Masui, X. H. Wu, B. Heying, J. S. Speck, U. K. Mishra, and S. P. DenBaars, J. Electron. Mater. **24**, 1707 (1995).
[19] Y.-H. Cho, F. Fedler, R. J. Hauenstein, G. H. Park, S. Keller, U. K. Mishra, and S. P. DenBaars, J. Appl. Phys. **85**, 3006 (1999).
[20] A. M. Witowski, K. Pakula, J. M. Baranowski, M. L. Sadowski, and P. Wyder, Appl. Phys. Lett. **75**, 4154 (1999).
[21] J. I. Pankove, S. Bloom, and G. Harbeke, RCA Rev. **36**, 163 (1975).
[22] C. P. Foley and T. L. Tansley, Phys. Rev. B **33**, 1430 (1986).
[23] A. J. Fischer, W. Shan, J. J. Song, Y. C. Chang, R. Horning, and B. Goldenberg, Appl. Phys. Lett. **71**, 1981 (1997).
[24] G. Martin, A. Botchkarev, A. Rockett, and H. Morkoç, Appl. Phys. Lett. **68**, 2541 (1996).
[25] D. A. B. Miller, D. S. Chemla, T. C. Damen, A. C. Gossard, W. Wiegmann, T. H. Wood, and C. A. Burrus, Phys. Rev. B **32**, 1043 (1985).
[26] C. K. Choi, B. D. Little, Y. H. Kwon, J. B. Lam, J. J. Song, Y. C. Chang, S. Keller, U. K. Mishra, and S. P. DenBaars, Phys. Rev. B **63**, 195 302 (2001).
[27] T. Takeuchi, C. Wetzel, S. Yamaguchi, H. Sakai, H. Amano, I. Akasaki, Y. Kaneko, S. Nakagawa, Y. Yamaoka, and N. Yamada, Appl. Phys. Lett. **73**, 1691 (1998).
[28] E. Cohen and M. D. Sturge, Phys. Rev. B **25**, 3828 (1982).
[29] S. Permogorov and A. Reznitsky, J. Lumin. **52**, 201 (1992).
[30] C. Gourdon and P. Lavallard, Phys. Status Solidi B **153**, 641 (1989).
[31] M. Oueslati, C. Benoit la Guillaume, and M. Zouaghi, Phys. Rev. B **37**, 3037 (1988).
[32] R. C. Miller, D. A. Kleinman, W. T. Tsang, and A. C. Gossard, Phys. Rev. B **24**, 1134 (1981).
[33] G. Bastard, E. E. Mendez, L. L. Chang, and L. Esaki, Phys. Rev. B **26**, 1974 (1982).
[34] W. Götz, N. M. Johnson, C. Chen, H. Liu, C. Kuo, and W. Imler, Appl. Phys. Lett. **68**, 3144 (1996).